A new Gaussian MCTDH program: Implementation and validation on the levels of the water and glycine molecules

D. Skouteris, and V. Barone

Citation: J. Chem. Phys. **140**, 244104 (2014); doi: 10.1063/1.4883677
View online: https://doi.org/10.1063/1.4883677
View Table of Contents: http://aip.scitation.org/toc/jcp/140/24
Published by the American Institute of Physics

A new Gaussian MCTDH program: Implementation and validation on the levels of the water and glycine molecules

D. Skouteris[a] and V. Barone[b]
Scuola Normale Superiore, Piazza dei Cavalieri 7, I-56126 Pisa, Italy

(Received 25 March 2014; accepted 4 June 2014; published online 24 June 2014)

We report the main features of a new general implementation of the Gaussian Multi-Configuration Time-Dependent Hartree model. The code allows effective computations of time-dependent phenomena, including calculation of vibronic spectra (in one or more electronic states), relative state populations, etc. Moreover, by expressing the Dirac-Frenkel variational principle in terms of an effective Hamiltonian, we are able to provide a new reliable estimate of the representation error. After validating the code on simple one-dimensional systems, we analyze the harmonic and anharmonic vibrational spectra of water and glycine showing that reliable and converged energy levels can be obtained with reasonable computing resources. The data obtained on water and glycine are compared with results of previous calculations using the vibrational second-order perturbation theory method. Additional features and perspectives are also shortly discussed. © *2014 AIP Publishing LLC*. [http://dx.doi.org/10.1063/1.4883677]

I. INTRODUCTION

In the last decades, quantum dynamics has become a routine tool for studying dynamical processes of atomic and molecular systems. Even though the use of classical mechanics in the study of the nuclear motion (coupled with simple schemes, such as the Landau-Zener model, for the treatment of electronically nonadiabatic processes) furnishes a qualitatively and sometimes quantitatively satisfactory picture, effects such as tunnelling, resonances, and zero point energy can only be completely accounted for through the use of quantum mechanical calculations.

Exact quantum dynamics calculations, both from a time-independent and a time-dependent point of view, have been used with success in the treatment of three- and four-atom systems, particularly in the study of chemical reactivity at the level of reaction probabilities and cross-sections. However, it is a fact that both CPU time and memory requirements increase exponentially with the number of degrees of freedom (DOF) of the system. As a result, with the current computing capabilities, exact calculations cannot be carried out for more than four or (in favorable cases, e.g., light atoms) five atom systems. Approximate schemes need to be devised in order to treat chemically interesting systems of higher dimensionality.

The multi-configuration time-dependent Hartree (MCTDH) scheme[1] has been demonstrated to be a valid approach to the quantum treatment of high-dimensional systems. Its central concept lies in the decomposition of the wavefunction into a linear combination of products (*configurations*) of wavefunctions of lower dimensionality. Both the expansion coefficients and the lower dimensionality functions evolve in time and this permits the adequate representation of the system.

One weakness of the MCTDH scheme is the necessity of a pre-fitted potential energy surface (PES) which, moreover, in order to be utilisable in a MCTDH calculation (unless schemes such as correlation discrete variable representation are used) needs to be decomposed in MCTDH form[1] (with negative repercussions to its accuracy). The complete calculation and fitting of a PES for a high dimensional system, however, is normally prohibitively expensive and one would like a method which permits calculations "on the fly," determining *ab initio* points only where needed.

The Gaussian MCTDH (G-MCTDH) scheme provides such a method. Gaussian wavefunctions possess a naturally localized structure which provides a classical-like picture of the evolving dynamics and their trajectories offer a natural indication of the configuration space spanned by the dynamics. Gaussian wavepacket (henceforth referred to as GWP) representation was pioneered by Heller[2,3] who made extensive use of Gaussians for various quantum dynamics problems. Sawada and Metiu[4] utilised a GWP to study curve crossing problems through a multiple trajectory theory. In 1999, Burghardt *et al.*[5] formulated the GWP representation in terms of the already successful MCTDH scheme, expressing the equations of motion as a generalization of the MCTDH ones (both within the wavefunction and the more general density matrix formalism). The first application of this method was performed by Worth and Burghardt[6] on a four-dimensional Henon-Heiles potential surface. The method was subsequently used in studying the dynamics of butadiene,[8] nitrosyl chloride,[9,10] pyrazine,[13] and benzene.[12] Moreover, Shalashilin and Burghardt presented a formulation of the method in terms of trajectories of coupled classical and quantum variables[7] and Mendive-Tapia *et al.*[14] have applied frozen-width variational Gaussian functions to study the nonadiabatic dynamics of fulvene. In general, the use of direct dynamics with coupled Gaussian trajectories is termed the direct-dynamics variational multi-configuration

[a]Author to whom correspondence should be addressed. Electronic mail: dimitrios.skouteris@sns.it
[b]Electronic mail: vincenzo.barone@sns.it

Gaussian method (DD-vMCG). A review and comparison of direct dynamics methods can be found in Ref. 11. Recently, Römer *et al.* have begun formulating a two-layer approach of the method (parallelling the highly promising multilayer MCTDH (ML-MCTDH) scheme).[15] A trajectory-guided variant of the method (coupled coherent states or CCS) has recently been compared to the standard variational Gaussian method against a number of benchmarks.[16] Within the context of direct dynamics methods, the *ab initio* multiple spawn (AIMS)[17–19] method as well as the *ab initio* multiconfiguration Ehrenfest (AI-MCE)[20] deserve mention.

Even though the G-MCTDH method has been established as a valid tool in quantum dynamical calculations, one still has to rely on benchmark calculations to assess the accuracy of the results, both as a function of the numbers of Gaussians used per degree of freedom and in terms of the mode combination pattern utilised. It would be highly desirable if a method were available to obtain an estimate of the truncation error introduced by the use of the evolving basis set (instead of the use of the time-dependent Schrödinger equation with no basis set contraction). We have recently developed a fully general G-MCTDH code which uses the constant mean field (CMF) approach in its propagation. Moreover, we have devised a way of estimating the truncation error introduced through the use of propagating Gaussians. In this paper, we present a series of preliminary results on the vibrational spectra of various simple systems. We stress that even though the following calculations are performed on a single potential energy surface, our program is fully equipped to deal with the multisurface case (assuming a diabatic representation of the different states). In this case, during a calculation "on-the-fly," not only the energies but also the coupling elements between the states should be provided.

The paper is organized as follows. In Sec. II, we present the general properties of the MCTDH and G-MCTDH scheme (the interested reader can find more detailed expositions in Ref. 1) as well as some specific numerical aspects of our code. In Sec. III, we present some preliminary results for selected 1D anharmonic oscillators as well as the H_2O and glycine molecules and discuss them. Section IV concludes.

II. THEORY AND NUMERICAL DETAILS

A. The G-MCTDH scheme

The G-MCTDH scheme can be seen as a special case of the MCTDH evolution scheme.[21–24] More information on the original Gaussian dynamics formulation can be found in Refs. 2 and 3. Details on the G-MCTDH scheme (expounded below) can be found in Refs. 5, 6, and 8. Within the MCTDH scheme the overall wavefunction is written in the form

$$\Psi = \sum_J A_J G_J, \tag{1}$$

where the A_J are complex coefficients and the G_J are *configurations*,

$$G_J = \prod_{i=1}^{d} g_J^{(i)}(\phi_i). \tag{2}$$

In the last equation, ϕ_i denotes the ith *logical coordinate* of the system, comprising one or more physical coordinates (in the latter case one speaks of *mode combination*). Moreover, $g_J^{(i)}$ is the *single particle function* (SPF) pertaining to the Jth configuration and the ith logical coordinate. In the specific case of G-MCTDH, the single particle functions are Gaussian functions whose width can be fixed (frozen Gaussians) or variable (thawed Gaussians). In the special case where all physical coordinates have been grouped together into one logical coordinate (and thus the wavefunction is represented as a linear combination of different trajectories, each with its coefficient, in the entire phase space), one obtains the so-called *variational multi-configuration Gaussian (v-MCG)* scheme. It is to be understood that, when the number of configurations is the rate-limiting factor in the calculation, the v-MCG scheme is to be preferred. In that case, full use is made of the separate configurations and the variational space spanned is maximised.

Another way of writing the wavefunction is

$$\Psi = \sum_{i=1}^{s_d} \Psi_i^{(d)} g_i^{(d)}, \tag{3}$$

where d is any logical coordinate (comprising s_d SPFs), $g_i^{(d)}$ is the ith SPF, and $\Psi_i^{(d)}$ is termed the ith *single hole function* for the dth logical coordinate.

The time evolution of the wavefunction is determined by the Dirac-Frenkel variational principle:

$$\left\langle \delta\Psi \middle| \hat{H}\Psi - i\frac{\partial \Psi}{\partial t} \right\rangle = 0, \tag{4}$$

which, essentially, states that any deviation from the time-dependent Schrödinger equation should be orthogonal to the variational tangent space of the wavefunction. It should be noted that, in the G-MCTDH scheme (contrary to standard MCTDH) the SPFs are generally not orthonormal and this complicates the evolution equations. The coefficients A_J (expressed as the $N \times 1$ vector $\boldsymbol{A}$, where N is the number of configurations) evolve according to the equation

$$i\boldsymbol{S}\dot{\boldsymbol{A}} = (\boldsymbol{H} - i\boldsymbol{\tau})\boldsymbol{A}. \tag{5}$$

Here $\boldsymbol{S}$ is the $N \times N$ configuration overlap matrix defined by $S_{JJ'} \equiv \langle G_J | G_{J'} \rangle$, $\boldsymbol{H}$ is the $N \times N$ Hamiltonian matrix defined by $H_{JJ'} \equiv \langle G_J | H | G_{J'} \rangle$ and $\boldsymbol{\tau}$ is the $N \times N$ differential overlap matrix defined by $\tau_{JJ'} \equiv \langle G_J | \partial_t G_{J'} \rangle$ (∂_t denotes time differentiation).

On the other hand, the Gaussian parameters λ (expressed through the vector $\boldsymbol{\Lambda}^{(d)}$) evolve according to the equation

$$i\boldsymbol{C}^{(d)}\dot{\boldsymbol{\Lambda}}^{(d)} = \boldsymbol{Y}^{(d)}. \tag{6}$$

The $\boldsymbol{C}^{(d)}$ matrix ($n_d \times n_d$, where n_d is the total number of Gaussian parameters for the logical coordinate d) is given by the expression

$$C_{j\lambda, j'\lambda'} = \rho_{jj'}^{(d)} \langle \partial_\lambda g_j | 1 - P^{(d)} | \partial_{\lambda'} g_{j'} \rangle. \tag{7}$$

Here ρ is the density matrix, defined by $\rho_{jj'}^{(d)} = \langle \Psi_j^{(d)} | \Psi_{j'}^{(d)} \rangle$ and $P^{(d)}$ is the projection operator on the space

spanned by the (non-orthonormal) SPFs of the dth logical coordinate:

$$P^{(d)} = \sum_{i,j} |g_i^{(d)}\rangle (S^{-1})_{ij} \langle g_j^{(d)}|. \quad (8)$$

The $n_d \times 1$ vector $\boldsymbol{Y}^{(d)}$ is given by the equation

$$Y_{j\lambda} = \sum_{j'} \langle \partial_\lambda g_j | (1 - P^{(d)}) H^{mf,d}_{jj'} | g_{j'} \rangle, \quad (9)$$

where $H^{mf,d}_{jj'} = \langle \Psi^{(d)}_j | \hat{H} | \Psi^{(d)}_{j'} \rangle$ is the j, j' component of the mean field Hamiltonian operator for the dth logical coordinate.

It has been noted by various authors that the use of thawed Gaussians causes numerical instabilities. We have thus chosen, within our code, to use exclusively frozen Gaussians. For each logical coordinate d composed of n_d physical coordinates, each SPF is of the form

$$g_i^{(d)}(\phi^{(d)}) = N_i^{(d)} \prod_{i=1}^{n_d} \exp\left(- a_i^{(d)} \phi_i^{(d)2} + b_i^{(d)} \phi_i^{(d)} \right). \quad (10)$$

The $a_i^{(d)}$ are real, positive constants that define the width of the Gaussians, whereas the $b_i^{(d)}$ parameters express the center of each Gaussian in phase space, the peak position (q), and momentum (p) of each Gaussian being given by the relations

$$\mathrm{Re}\left(b_i^{(d)}\right) = -2a_i^{(d)} q, \quad (11)$$

$$\mathrm{Im}\left(b_i^{(d)}\right) = p. \quad (12)$$

Thus, for a frozen Gaussian, the only varying parameter is $b_i^{(d)}$. The normalization factor $N_i^{(d)}$ is chosen so that each SPF is normalized. The advantage of keeping all Gaussians normalized lies in the fact that, in this case, the modulus of the overlap integral of each pair of Gaussians decreases monotonically as the two functions move farther away from each other, either in coordinate or in momentum space. It would, therefore, seem natural to include also the $N_i^{(d)}$ factors in the list of variationally optimized parameters. However, the normalization factor cannot be treated as an independent parameter within the Dirac-Frenkel variation scheme because it contains the square of the real part of b and thus the overall SPF would no longer be an analytic function of b. As a result, within a single time step, the Gaussians are propagated with no assumption of normalization. At the end of each time step, all coefficients A_J are modified according to the new positions of the Gaussians so that the latter ones are normalized.

B. The local harmonic approximation (LHA)

As stressed above, the G-MCTDH approach is promising because of its potential to be used in calculations "on the fly," without using a pre-fitted potential energy surface. The commonly used approach in such calculations is the local harmonic approximation. Within this scheme, the potential energy is locally approximated using its value, its derivative vector and its Hessian matrix around each configuration point. We have used this scheme, utilising the fact that the product of two Gaussians of the same width is a Gaussian whose coordinate peak lies exactly in the middle of the two, its momentum peak is equal to the difference of the two momenta and its height is a Gaussian function of the distance in phase space. Since what interests us is the potential matrix element between *two* configurations, at each time step we evaluate the potential (V), the derivative vector (V_a) and the Hessian matrix (V_{ab}) at the peak position of each configuration and subsequently we use the formulae

$$V_{mid} = \frac{1}{2}(V_1 + V_2) - \frac{5}{32} \sum_a (V_{1,a} - V_{2,a}) \delta x^{(a)} + \frac{1}{64} \sum_{a,b} (V_{1,ab} + V_{2,ab}) \delta x^{(a)} \delta x^{(b)} + O(h^6), \quad (13)$$

$$V_{mid,a} = \frac{1}{2}(V_{1,a} + V_{2,a}) - \frac{1}{8} \sum_b (V_{1,ab} - V_{2,ab}) \delta x^{(b)} + O(h^4), \quad (14)$$

$$V_{mid,ab} = \frac{1}{2}(V_{1,ab} + V_{2,ab}) + O(h^2), \quad (15)$$

where h is the total distance between the two points. It is easy to verify that these formulae are exact for up to a cubic potential.

C. The constant mean field scheme

In standard MCTDH calculations, a substantial simplification is introduced through the constant mean field scheme (CMF). Within this scheme, the Hamiltonian matrix as well as the density and mean field matrices are assumed to be constant within a single time step. This assumption is justified by the fact that the variation of these quantities is usually much slower than that of the coefficients and SPFs and therefore one can afford to use a longer time step. More information about the CMF scheme can be found in Refs. 1 and 25.

In the G-MCTDH scheme, we use the same CMF approximation. We assume that both the Hamiltonian and S matrices are constant within a time step, as both of them contain configuration products of Gaussians (with no coefficients) whose time variation, assuming no correlation between them, is likely to partially cancel out. We have verified that this is indeed the case in test calculations. The only problematic case is when two configurations approach each other too closely in phase space, rendering the S matrix near-singular. At each point in time, the S matrix is stabilised using well-known methods[1] in order to avoid problems due to such singularities. Subsequently, the A_J coefficients are propagated using an ordinary Arnoldi scheme.

The propagation of the Gaussian parameters is more complicated, as the relevant equations are nonlinear due to the presence of the projection operator. In our code, we assume that the density matrix remains constant within a time step. Each mean field operator, within the LHA and due to the particular form of the Gaussian functions, can be written as a second degree polynomial in the relevant physical coordinates and, in our version of the CMF scheme, we assume the coefficients of this polynomial to be constant. Subsequently, the parameters are propagated using a fourth order Runge-Kutta scheme.

D. The effective Hamiltonian

In general, when the Dirac-Frenkel principle is used to propagate a wavefunction, a system of equations of the form

$$\langle \partial_\lambda \Psi | \hat{H} | \Psi \rangle = i \langle \partial_\lambda \Psi | \dot{\Psi} \rangle \tag{16}$$

is generated for each parameter λ which, using the chain rule, is transformed to

$$i \sum_\mu \langle \partial_\lambda \Psi | \partial_\mu \Psi \rangle \frac{d\mu}{dt} = \langle \partial_\lambda \Psi | \hat{H} | \Psi \rangle. \tag{17}$$

Thus, defining the matrix $\boldsymbol{D}$ and the vector $\boldsymbol{K}$ by the equations

$$\begin{aligned} D_{\lambda\mu} &= \langle \partial_\lambda \Psi | \partial_\mu \Psi \rangle, \\ K_\lambda &= \langle \partial_\lambda \Psi | \hat{H} | \Psi \rangle, \end{aligned} \tag{18}$$

respectively, the evolution equations (for the parameter vector $\boldsymbol{\Lambda}$) turn out to be

$$i \dot{\boldsymbol{\Lambda}} = \boldsymbol{D}^{-1} \boldsymbol{K} \tag{19}$$

and the effect on the overall wavefunction is

$$i |\dot{\boldsymbol{\Psi}}\rangle = \sum_{\lambda,\mu} |\partial_\lambda \Psi\rangle (\boldsymbol{D}^{-1})_{\lambda\mu} \langle \partial_\mu \Psi | \hat{H} | \Psi \rangle = P_e \hat{H} | \Psi \rangle, \tag{20}$$

where P_e is the projection operator on the space spanned by the $|\partial_\lambda\rangle$ kets. Thus, it is seen that the Dirac-Frenkel evolution equation can be written as a time-dependent Schrödinger equation but with an effective Hamiltonian

$$\hat{H}_{eff} = P_e \hat{H}. \tag{21}$$

There are various observations one can make on this equation. First of all, since P_e itself depends on the wavefunction Ψ, the effective Hamiltonian is no longer time-independent and the corresponding TDSE is no longer linear. Moreover, the effective Hamiltonian is in general non-Hermitian since P_e does not commute with $\hat{H}$ (even though both are Hermitian). Indeed, for a general set of evolving parameters the wavefunction norm is not conserved (but, as we show in the Appendix, the total energy is conserved). However, if one of the parameters is an overall multiplier of the wavefunction, then $|\Psi\rangle$ itself belongs to the space spanned by the $|\partial_\lambda\rangle$ kets and hence $P_e|\Psi\rangle = |\Psi\rangle$. Thus, the non-Hermitian Hamiltonian can be replaced by the Hermitian one $P_e \hat{H} P_e$ and thus the norm is conserved. Note that the projection operator P_e is *not* the same as the projection operator $P^{(d)}$ that appears in the parameter evolution equations but, in the case of v-MCG (one logical coordinate), the latter operator projects only on a proper subspace of P_e. For the G-MCTDH scheme (with frozen Gaussians), P_e projects on the subspace spanned by

- The configuration kets $|G_J\rangle$;
- The kets of the form $|\Psi_i^{(d)}\rangle |\partial_b g_i^{(d)}\rangle$ for each logical coordinate d.

This subspace (assuming complete linear independence) has a dimension of $N_J + \sum_d N_d$ where N_J is the number of configurations and N_d is the number of SPFs for the logical coordinate d.

This result suggests a way to estimate the representation error introduced through the use of the G-MCTDH scheme. As the wavefunction evolves under the effective Hamiltonian $P_e \hat{H}$, a time-dependent perturbation to the true Hamiltonian $\hat{H}$ is introduced, equal to $\hat{H}_p = (\hat{1} - P_e)\hat{H}$. The norm of the ket $|\phi\rangle = (\hat{1} - P_e)\hat{H}|\Psi\rangle$ thus gives an upper bound to the error in the wavepacket time derivative.

III. RESULTS AND DISCUSSION

A. The 1D Morse, polynomial, and double Morse oscillators

In order to illustrate how the width and the number of Gaussians employed can affect the calculation in practice, we have performed some simple calculations on the spectrum of some one-dimensional anharmonic oscillators, calculating the error in the effective Hamiltonian at each step.

One feature of our code is the option to perform variational, time-independent calculations on the provided Gaussian basis set in order to estimate the stationary energy levels of the system. This way, we use time-independent Gaussian functions (propagating only the coefficients in time) and we can afford to use many more Gaussians than in a calculation where time-dependent dynamics is more important than spectra. The calculation proceeds as follows. At each time step, we calculate the autocorrelation function of the wavepacket,

$$\phi(t) = \langle \psi(0) | \psi(t) \rangle. \tag{22}$$

The spectrum of the vibrational levels represented in the initial wavepacket can then be calculated through the half-Fourier transform,

$$s(E) \propto \mathrm{Re}\left(\int_0^\infty \phi(t) e^{iEt/\hbar} dt \right). \tag{23}$$

In principle, the width of the Gaussians utilised in the calculation is an arbitrary parameter, since, with enough Gaussians included, the exact results will be obtained. Both in this and in subsequent cases, the vibrational spectra have been calculated at a temperature of 0 K. Since imaginary time propagation is an option in our code, vibrational spectra at higher temperatures can also be calculated. The height of each peak (corresponding to a particular vibrational level) depends on the initial wavepacket used. In this work, it is arbitrary but, in general, the initial wavepacket can be the product of the transition dipole moment and the vibrational ground state wavefunction. In this case, one gets the vibrational spectrum. Moreover, our code permits the use of multiple interacting electronic states in the propagation.

It is to be noted that, in the case of a 1D oscillator (and, more generally, in the case of a v-MCG calculation, where each Gaussian parameter is employed in exactly one configuration), the constant and linear parts of the Hamiltonian do not have to be included in the error expression since for these parts we have $(\hat{1} - P_e)H = 0$. In fact, only the quadratic terms (within the LHA), both from the potential and the kinetic energy part of the Hamiltonian, contribute to the error.

The oscillators used in the present case have unit mass and a force constant at the equilibrium point of 10^{-4}

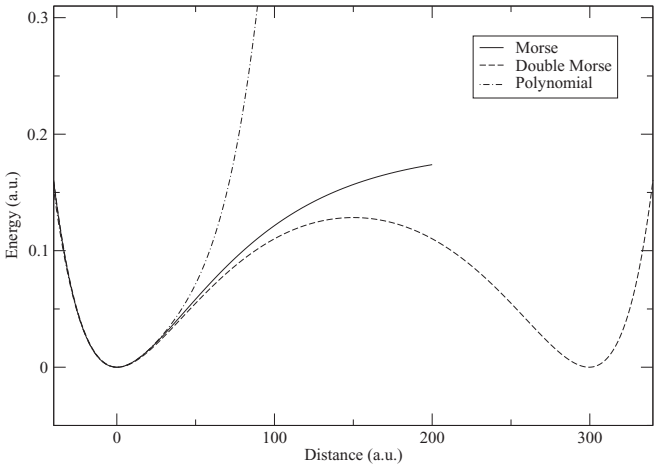

FIG. 1. Potential energy curves representing the Morse, double Morse and polynomial potentials.

atomic units. In terms of the potentials, the three oscillators comprise:

1. A Morse oscillator (MO), with constants $D_e = 0.188$ hartree and $\beta = 0.0163\ a_0^{-1}$;
2. A double Morse oscillator (DMO), which is the sum of two Morse oscillators with the same constants and a separation of 300 a_0 between the minima;
3. A polynomial oscillator (PO), with the same derivatives at the minimum (up to the fourth one) as the Morse oscillator.

The three potential energy curves can be seen in Fig. 1. With this mass and force constant, for a harmonic oscillator, the error would vanish (the kinetic energy and the potential energy error terms exactly cancel each other out) for a width parameter of the Gaussian $a = 10\ a_0$. We have performed a calculation of the energy spectrum using one single Gaussian, starting at a distance of 40.0 a_0, with parameters of 10, 5, and 2 a_0. We present the results in Figs. 2–4.

In Fig. 2 are shown the paths (in phase space) of calculations for the three oscillators involving a single Gaussian (the

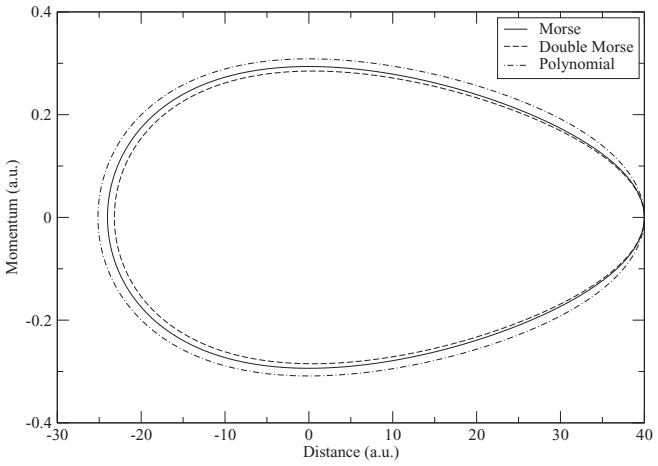

FIG. 2. Phase space paths of single Gaussian calculations for the three potentials starting from a distance of 40.0 a_0.

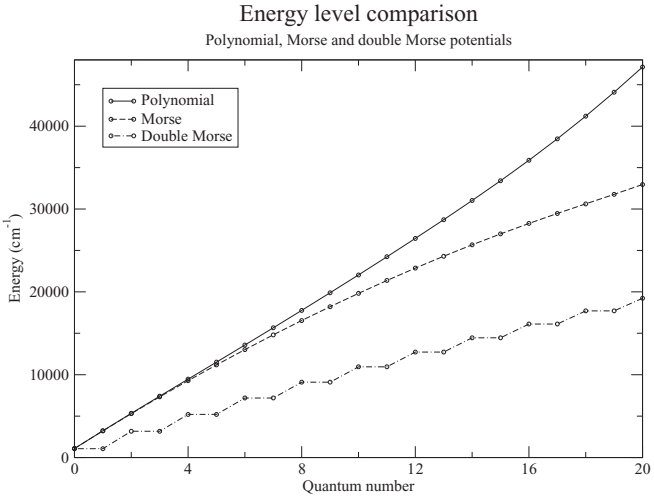

FIG. 3. Comparison of energy level spectra (of quantum numbers going up to 20) for the three 1D oscillators, obtained through propagation of immobile Gaussians.

calculation was repeated for the various widths but the results are virtually identical). In conjunction with the curves shown in Fig. 1 and the essentially classical nature of the propagation, it can be seen that the polynomial trajectory is the one with the highest amount of energy (reaching the minimum distance in the repulsive region), followed by the Morse and the double Morse ones.

In Fig. 3 are shown the lowest 20 energy levels for each of the three 1D oscillators. These levels have been obtained by a calculation using time-independent Gaussians (where only the coefficients were propagated in time). This has allowed us to use a high number of Gaussians thus better representing the levels. Specifically, we have used 86 SPFs for the MO, 191 for the DMO (many more because of the extended nature of the double well) and 56 for the PO. In the case of the DMO, the almost perfect double degeneracy of the levels can be seen (in all cases the tunnelling splitting remains below 10^{-6} cm^{-1}). Furthermore, each doublet has almost the

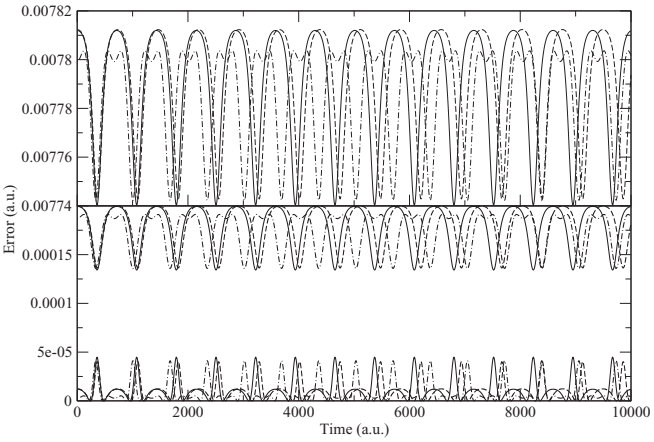

FIG. 4. Propagation of truncation errors (in inverse square atomic time units) for all three 1D oscillators and Gaussian widths of 10.0 a_0, 5.0 a_0 (shown in lower portion) and 2.0 a_0 (shown in higher portion). In all three cases, the Morse oscillator is denoted by the solid line, the double Morse oscillator by the dashed line, and the polynomial oscillator by the dotted-dashed line.

same energy as a corresponding level of the other two oscillators. The MO and PO start off with essentially equal values of their energy levels (as expected, since the two potentials agree up to the fourth derivative). Differences between the two start becoming apparent at a quantum number of around 4. Already at a quantum number of $n = 2$, there is a difference of 30 cm^{-1} between the two cases, rising to 180 cm^{-1} for $n = 4$ and around 300 cm^{-1} for $n = 5$. We believe that this result illustrates the danger of too much confidence in a polynomial approximation of a potential away from the equilibrium point. In this case, the approximation is a fourth order one but the same argument can be carried over for higher orders. This is a very strong point to be made for seeking alternative methods of approximating the potentials (with a view to simulating the correct asymptotic behavior) and we are currently working along this line.

In Fig. 4 are shown the truncation error curves for the three potentials and the three Gaussian widths. Because of the large difference, the portion pertaining to the 2.0 a_0 width has been separated from the rest (in the upper portion) whereas the other two cases are shown in the lower portion. As the three cases are well separated, we have chosen to always assign a solid line to the MO, a dashed line to the DMO and a dotted-dashed line to the PO. It is seen that the 10.0 a_0 case is always the one with the lowest error and this can be understood as a consequence of the fact that this is the width corresponding to the harmonic oscillator of the same force constant (given generally by the formula $x = \sqrt{\frac{\hbar}{m\omega}}$). As the width diminishes, the truncation error (due to the fact that the Gaussians are constrained to be frozen) correspondingly increases. In all cases, the structure of the error curves is periodic, reflecting the periodic nature of the corresponding trajectories (in fact, all curves pertaining to the PO have noticeably shorter periods reflecting the shorter period of the corresponding trajectories). However, there are interesting differences among the three Gaussian widths.

In the case of the 10.0 a_0 width, the instantaneous error has local maxima at the oscillator extremes and (zero) minima between them. The zero instantaneous error is obviously caused by the fact that, when the Gaussian passes through the minimum it has the correct coherent length for the corresponding local oscillator and the propagation is locally exact. As the second derivative changes at the extremes (more so for the repulsive region), this is reflected in the error. The other two cases show a maximal error at the maximum distances and a monotonic diminution of the error until a minimal error is reached at the minimum distance. In both cases, the error is diminished as the local force constant increases (and the corresponding coherent width approaches that of the Gaussian). In particular, for the DMO case, a small shoulder structure is seen indicating a point where the potential third derivative becomes 0.

B. Simple molecules

Although the possibility to perform on-the-fly computations is one of the strengths of the G-MCTDH approach, in our first validation we have chosen to use harmonic and anharmonic force fields computed by density functional theory (DFT) using our finite difference implementation[26] in the GAUSSIAN package.[27] Among other things, this choice allows direct comparison with the second order perturbative approach (VPT2) available in the same code.[28–31] In particular, we have made use of the double-hybrid B2PLYP functional[32–34] and the aug-cc-pVTZ basis set, in view of previous experience about the reliability of this computational model.[34–36]

1. The H_2O energy levels

We have tested our algorithm calculating the positions of the vibrational energy levels of the H_2O molecule within the harmonic approximation. As usual, we set up an initial wavepacket for the H_2O molecule and we follow its evolution in time.

In all cases, the initial state of the H_2O molecule is given by a product of Gaussian wavepackets. In the cases when one wavepacket is used in a physical degree of freedom, this is peaked at a value of the mass-weighted normal coordinate of 10.0 a.u. When two wavepackets are used, they are peaked at 10.0 a.u. and 4.0 a.u. In the case of the v-MCG calculation, the two SPFs are composed of Gaussian wavepackets either all centered at 4.0 a.u. or 10.0 a.u. Information on the widths of the wavepackets follows.

We have carried out two different types of calculations on the H_2O molecule, either combining all three vibrational motions into one logical coordinate (v-MCG calculations) or treating each as a logical coordinate in its own right (standard G-MCTDH). In all, four types of calculations have been performed:

1. Single configuration calculations, where the Gaussian widths for each of the three modes are optimal;
2. Single configuration calculations, where the Gaussian width for each of the three modes is 10 a_0 (non-optimal);
3. v-MCG calculations, with a width of 10 a_0 for each mode, with two configurations;
4. Standard G-MCTDH calculations, with a width of 10 a_0 and two Gaussian SPFs for each mode (which makes for $2^3 = 8$ configurations in total).

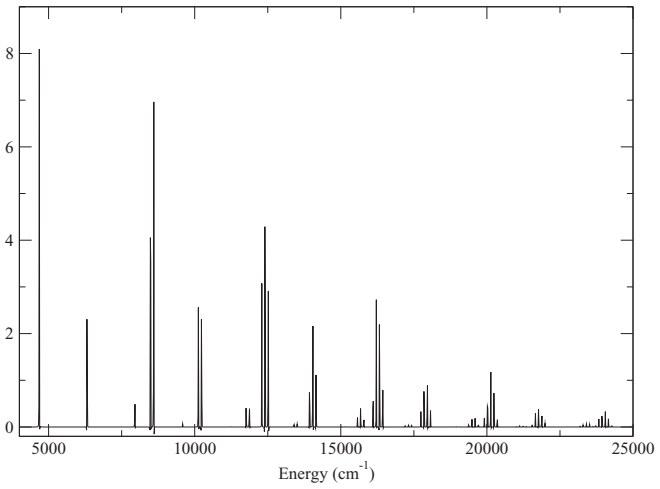

FIG. 5. Harmonic energy levels for the H_2O molecule obtained by propagation of one Gaussian SPF.

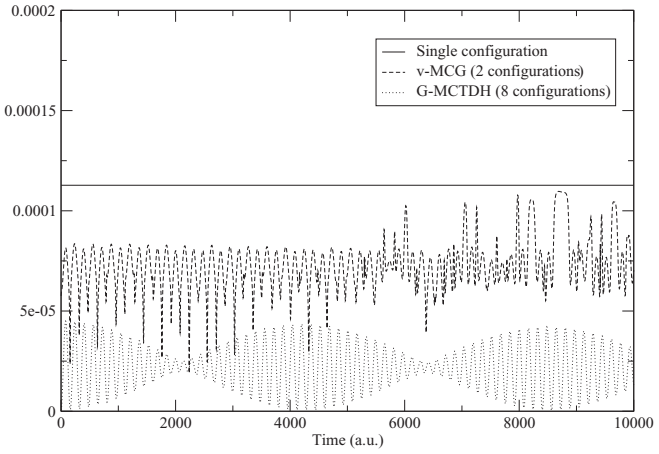

FIG. 6. Representation errors (in inverse square atomic time units) for the H_2O molecule propagation (with one Gaussian SPF).

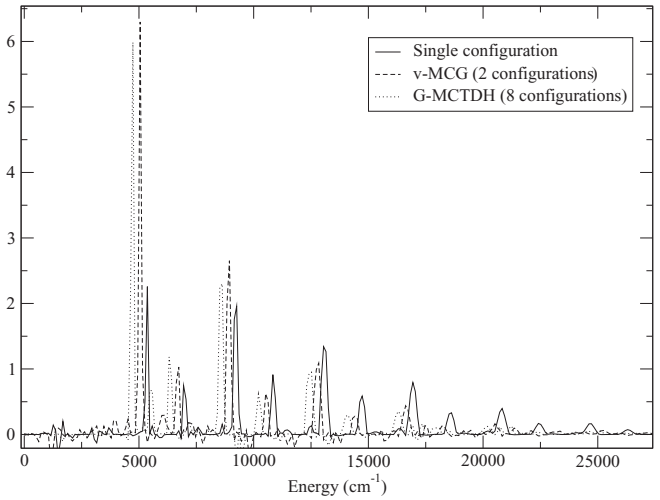

FIG. 7. Harmonic spectra of H_2O molecule for various types of calculations (single Gaussian, v-MCG with two Gaussian SPFs and G-MCTDH with two Gaussian SPFs for each of the three vibrational modes).

As expected, the error of the calculation in case 1 is zero and the exact vibrational levels of H_2O are obtained (in the harmonic approximation) using a single configuration, as shown in Fig. 5.

In Fig. 6 are shown the errors for the cases 2 to 4 of the previous list. The error decreases as the number of configurations increases and, as with the case of the 1D harmonic oscillator, its time-dependence acquires an oscillatory character when more than one configuration is considered. As before, the presumable origin of this behavior is due to the time-dependence of the span of the Gaussians, being maximised when the span is minimised.

In Fig. 7 the effect of the representation error on the H_2O spectrum can be seen. It appears that, in general, a high representation error causes a consistent shift of the energy levels towards higher energies. In fact, the single configuration calculation shows a shifting of all peaks (with respect to the exact calculation) towards the right. Adding one more configuration (in the sense of one more quantum trajectory in a v-MCG calculation) corrects this error by about 50%, whereas including two SPFs for each physical degree of freedom (for a total of 8 configurations) essentially brings the peaks to their correct position. It is to be noted that the Gaussian width used here ($10\ a_0$) is very close to the optimal values of the H_2O modes and, presumably, more Gaussians would have been needed if our choice of width had been less fortunate.

In order to obtain accurate values for the anharmonic levels of the water molecule, we have used the possibility of keeping the Gaussians immobile (in all cases the rotation-vibration interaction is not taken into account). This is in the spirit of the coupled coherent states (CCS) approach,[7] where the Gaussians follow predetermined trajectories as opposed to evolving variationally. We have used 125 v-MCG configurations, corresponding to 5 Gaussians per degree of freedom, distributed along the vibrational coordinates. Table I collects the zero point and the fundamental vibrational levels of H_2O, both as calculated by our code (variationally, with the original Gaussian width but not position-optimized) and by GAUSSIAN (through VPT2 perturbation theory). In order to check the convergence, calculations have also been carried out with 6 Gaussian SPFs per degree of freedom (the calculations with 5 Gaussians per DOF are shown in parentheses). It can be seen that, in the harmonic case, deviations between our code and the perturbation approach are less than 5 cm^{-1} whereas the maximum difference in the anharmonic case is around 60 cm^{-1} for the symmetric stretch level. The last column in Table I contains accurate variational results for the H_2O levels (again, neglecting vibrational angular momentum). It can be seen that the Gaussian anharmonic ground state is actually *lower* in energy than the variational value. The only source of error that can account for such a trend is the use of the local harmonic approximation in the Gaussian calculation. It follows that, even though the LHA is an entirely satisfactory scheme for the study of dynamics, one should be very careful about using it to obtain high quality energy level spectra.

TABLE I. Fundamental water levels (cm^{-1}) obtained through diagonalisation of Gaussians and through the VPT2 method. The numbers in parentheses correspond to 5 Gaussians per mode, whereas the ones outside correspond to 6 Gaussians per mode.

Level	Harm (Gaussian)	Harm (exact)	Anharm (Gaussian)	Anharm (VPT2)	Variational
000	4680.96 (4680.98)	4680.93	4581.08 (4581.41)	4607.03	4613.73
100	6317.54 (6317.70)	6317.06	6167.28 (6168.75)	6187.72	6187.28
010	8492.16 (8493.47)	8488.68	8180.81 (8185.82)	8240.95	8291.25
001	8601.66 (8602.65)	8598.90	8372.00 (8384.41)	8338.92	8394.55

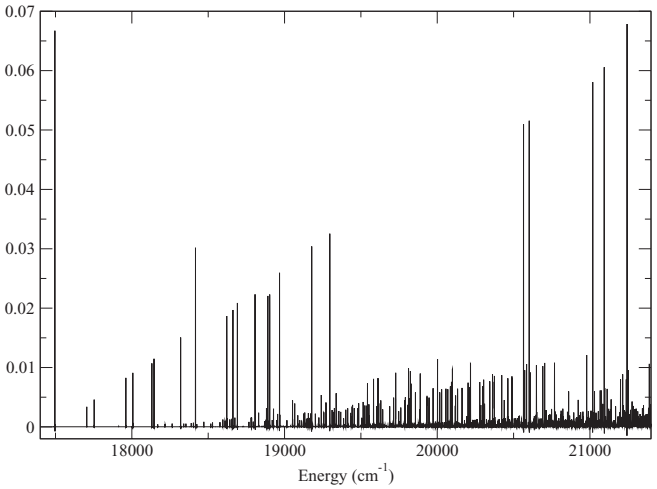

FIG. 8. Harmonic spectrum of the vibrational modes of the glycine molecule obtained by propagating one Gaussian SPF.

2. The glycine molecule

Moving towards a higher number of degrees of freedom, we have performed calculations on the glycine molecule. The first test is a harmonic calculation including 23 degrees of freedom (all but the C-C rotation), whose results are shown in Fig. 8 (as before, choosing appropriately the width of the Gaussians permits an exact propagation and an exact calculation of the energy levels). It can be seen that the pattern of intensities in the case of the fundamental levels is essentially linear with the transition frequency (energy difference from the ZPE). This is due to the localized nature of the initial wavepacket in which all 23 Gaussians peak at a mass-weighted normal coordinate of 10.0 a.u. In fact, it can be shown that if the initial wavepacket is much closer to the equilibrium point than the coherent distance scale of the oscillator, the square of its overlap with the $v = 1$ level is expected to vary linearly with the frequency.

We have chosen this particular system because its study is a natural continuation of the VPT2 and reduced dimensionality VPT2 calculations previously performed by our group.[28–31] As mentioned previously, such an approach necessitates the use of low width Gaussian functions in order not to compromise the local harmonic approximation. Nevertheless, one can observe that, for rigid systems undergoing low-amplitude motions a good estimate of their energy levels can be obtained through the time-independent framework. As was done also for the water molecule, here we present some results for the low-lying stretching levels of the glycine molecule. The calculation performed is a v-MCG one with 243 Gaussians (corresponding to 3 Gaussians per degree of freedom) distributed along the vibrational coordinates. Table II shows the ground and first excited stretching levels for glycine, both for the harmonic and the anharmonic case as calculated by our code and from VPT2 calculations. The zero point harmonic level falls exactly on the correct value (as the wavefunction of the corresponding level is represented exactly) while, in the anharmonic case, we have limited ourselves to comparing the transition frequency (which in both cases we have added to the zero point level calculated with the v-MCG method). The reason for this is that the zero point levels in the two cases (v-MCG and VPT2) take into account different numbers of vibrational modes and are thus not immediately comparable. In the worst case, the energy value is roughly 44 cm^{-1} off the true one. Bearing in mind that each level has had to be simulated with only three Gaussian functions, the approximation can again be judged satisfactory.

From the point of view of the G-MCTDH framework, the above time-independent calculations are equivalent to propagating only the coefficients of the configuration (i.e., keeping the Gaussian parameters constant). In this way, the necessity of the system to be semirigid can be appreciated—if the Gaussians do not move around the configuration space appreciably, varying only the coefficients can provide a good estimate of the energy levels. On the other hand, allowing mobile Gaussians increases the variational space (expands the P projection operator in the expression for the effective Hamiltonian) and can thus be expected to yield more accurate dynamics, especially for large amplitude motion.

IV. CONCLUSIONS

In this paper, we have presented our new G-MCTDH code for the study of time-dependent quantum dynamics of molecular systems and we have illustrated results for a sequence of systems of a progressively higher number of degrees of freedom. We have used the autocorrelation functions for 1D anharmonic oscillators of various kinds as well as the H_2O and the glycine molecules to obtain spectra of their respective vibrational energy levels and we have illustrated how our code can:

- Estimate the error due to the representation of the wavefunction as a linear combination of frozen Gaussians;
- Estimate variationally the lowest energy levels of relatively rigid systems.

TABLE II. Fundamental glycine levels (cm^{-1}) obtained through diagonalisation of Gaussians and through the VPT2 method.

Level	Harm (Gaussian)	Harm (exact)	Anharm (Gaussian)	Anharm (VPT2)
00000	8521.84	8521.84	8282.61	8282.61
10000	11593.85	11591.00	11219.40	11233.57
01000	11631.29	11628.43	11276.44	11243.20
00100	12047.79	12044.58	11636.82	11660.74
00010	12122.78	12119.51	11742.27	11709.59
00001	12272.79	12269.31	11887.22	11843.09

The latter item corresponds to propagating only the coefficients of the configurations and not the Gaussian parameters, an approximation which is expected to be good for the lowest levels of rigid systems. We point out that one can also choose an intermediate point between the two extremes and subject to the Dirac-Frenkel variational principle a proper subset of the Gaussian parameters (and/or the coefficients) and this is certainly the way to proceed as the number of rigid degrees of freedom increases (as is the case with Gaussian baths). For example, the Gaussian parameters can be chosen to evolve along a predetermined trajectory (e.g., determined by quasiclassical calculations) as is done in the coupled coherent states (CCS) method.[16] This is another option provided by our code.

Finally, in the case of problems of a much higher dimensionality (of the order of hundreds or thousands of DOFs) the algorithm is amenable to incorporation into a multilayer scheme.[15] In this case, each wavepacket of the form treated here would correspond to a single SPF of a single logical coordinate among many. A complete multilayer calculation would therefore consist of many such wavefunctions (orthonormal, as in the usual MCTDH scheme) coupled to analogous SPFs from other logical degrees of freedom and forming "superconfigurations," each one with its own coefficient.

ACKNOWLEDGMENTS

It is a pleasure to thank Matteo Piccardo and Ivan Carnimeo for the data supplied on H_2O and glycine, respectively. D.S. wishes to thank the European Research Council for a fellowship in the framework of the ERC Advanced Grant Project DREAMS "Development of a Research Environment for Advanced Modeling of Soft Matter," GA N. 320951.

APPENDIX: ENERGY CONSERVATION IN DIRAC-FRENKEL PROPAGATION

Here we show that the energy (the expectation value $\langle\Psi|\hat{H}|\Psi\rangle$) is always conserved when the Dirac-Frenkel principle is applied. Using the modified TDSE introduced in the text, we have

$$\frac{d}{dt}\langle\Psi|\hat{H}|\Psi\rangle = \langle\dot{\Psi}|\hat{H}|\Psi\rangle + \langle\Psi|\hat{H}|\dot{\Psi}\rangle. \quad \text{(A1)}$$

But since $|\dot{\Psi}\rangle = i\,P_e\hat{H}|\Psi\rangle$ and since both $\hat{H}$ and P_e are Hermitian, we get

$$\frac{d}{dt}\langle\Psi|\hat{H}|\Psi\rangle = \langle\Psi|\hat{H}\,P_e\hat{H}|\Psi\rangle - \langle\Psi|\hat{H}\,P_e\hat{H}|\Psi\rangle = 0, \quad \text{(A2)}$$

which is the desired result.

[1] M. H. Beck, A. Jäckle, G. A. Worth, and H.-D. Meyer, Phys. Rep. **324**, 1 (2000).
[2] E. J. Heller, J. Chem. Phys. **62**, 1544 (1975).
[3] E. J. Heller, J. Chem. Phys. **75**, 2923 (1981).
[4] S. Sawada and H. Metiu, J. Chem. Phys. **84**, 227 (1986).
[5] I. Burghardt, H.-D. Meyer, and L. S. Cederbaum, J. Chem. Phys. **111**, 2927 (1999).
[6] G. Worth and I. Burghardt, Chem. Phys. Lett. **368**, 502 (2003).
[7] D. V. Shalashilin and I. Burghardt, J. Chem. Phys. **129**, 084104 (2008).
[8] G. A. Worth, M. A. Robb, and I. Burghardt, Faraday Discuss. **127**, 307 (2004).
[9] B. Lasorne, M. J. Bearpark, M. A. Robb, and G. A. Worth, Chem. Phys. Lett. **432**, 604 (2006).
[10] B. Lasorne, M. A. Robb, and G. A. Worth, Phys. Chem. Chem. Phys. **9**, 3210 (2007).
[11] G. A. Worth, M. A. Robb, and B. Lasorne, Mol. Phys. **106**, 2077 (2008).
[12] B. Lasorne, M. J. Bearpark, M. A. Robb, and G. A. Worth, J. Phys. Chem. A **112**, 13017 (2008).
[13] I. Burghardt, K. Giri, and G. A. Worth, J. Chem. Phys. **129**, 174104 (2008).
[14] D. Mendive-Tapia, B. Lasorne, G. A. Worth, M. A. Robb, and M. J. Bearpark, J. Chem. Phys. **137**, 22A548 (2012).
[15] S. Römer, M. Ruckenbauer, and I. Burghardt, J. Chem. Phys. **138**, 064106 (2013).
[16] M. Ronto and D. V. Shalashilin, J. Phys. Chem. A **117**, 6948 (2013).
[17] T. J. Martinez, M. Ben-Nun, and R. D. Levine, J. Phys. Chem. **100**, 7884 (1996).
[18] M. Ben-Nun and T. J. Martinez, Adv. Chem. Phys. **121**, 439 (2002).
[19] A. M. Virshup, C. Punwong, T. V. Pogorelov, B. A. Lindquist, C. Ko, and T. J. Martinez, J. Phys. Chem. B **113**, 3280 (2009).
[20] D. V. Shalashilin, J. Chem. Phys. **132**, 244111 (2010).
[21] H.-D. Meyer, U. Manthe, and L. S. Cederbaum, Chem. Phys. Lett. **165**, 73 (1990).
[22] U. Manthe, H.-D. Meyer, and L. S. Cederbaum, J. Chem. Phys. **97**, 3199 (1992).
[23] H.-D. Meyer, U. Manthe, and L. S. Cederbaum, in *Numerical Grid Methods and Their Application to Schrödinger's Equation*, edited by C. Cerjan (Kluwer Academic Publishers, Dordrecht, 1993), pp. 141–152.
[24] U. Manthe, H.-D. Meyer, and L. S. Cederbaum, J. Chem. Phys. **97**, 9062 (1992).
[25] M. H. Beck and H.-D. Meyer, Z. Phys. D **42**, 113 (1997).
[26] V. Barone, J. Chem. Phys. **122**, 014108 (2005).
[27] M. J. Frisch, G. W. Trucks, H. B. Schlegel *et al.*, GAUSSIAN 09, Revision D.01, Gaussian, Inc., Wallingford, CT, 2009.
[28] V. Barone, M. Biczysko, J. Bloino, M. Borkowska-Panek, I. Carnimeo, and P. Panek, Int. J. Quantum Chem. **112**, 2185 (2012).
[29] I. Carnimeo, M. Biczysko, J. Bloino, and V. Barone, Phys. Chem. Chem. Phys. **13**, 16713 (2011).
[30] M. Biczysko, J. Bloino, I. Carnimeo, P. Panek, and V. Barone, J. Mol. Spectrosc. **1009**, 74 (2012).
[31] V. Barone, M. Biczysko, and J. Bloino, Phys. Chem. Chem. Phys. **16**, 1759 (2014).
[32] S. Grimme, J. Chem. Phys. **124**, 034108 (2006).
[33] F. Neese, T. Schwabe, and S. Grimme, J. Chem. Phys. **126**, 124115 (2007).
[34] M. Biczysko, P. Panek, G. Scalmani, J. Bloino, and V. Barone, J. Chem. Theory Comput. **6**, 2115 (2010).
[35] V. Barone, M. Biczysko, J. Bloino, and C. Puzzarini, Phys. Chem. Chem. Phys. **15**, 10094 (2013).
[36] I. Carnimeo, C. Puzzarini, N. Tasinato, P. Stoppa, A. P. Charmet, M. Biczysko, C. Cappelli, and V. Barone, J. Chem. Phys. **139**, 074310 (2013).